Suppression of surface segregation of the phosphorous δ-doping layer by insertion of an ultra-thin silicon layer for ultra-shallow Ohmic contacts on n-type germanium

Michihiro Yamada,[1] Kentarou Sawano,[2] Masashi Uematsu,[1] and Kohei M. Itoh[1,a)]
[1]*School of Fundamental Science and Technology, Keio University, 3-14-1 Hiyoshi, Kohoku-ku, Yokohama 223-8522, Japan*
[2]*Advanced Research Laboratories, Tokyo City University, 8-15-1 Todoroki, Setagaya-ku, Tokyo 158-0082, Japan*

(Received 2 June 2015; accepted 16 September 2015; published online 28 September 2015)

We demonstrate the formation of abrupt phosphorus (P) δ-doping profiles in germanium (Ge) by the insertion of ultra-thin silicon (Si) layers. The Si layers at the δ-doping region significantly suppress the surface segregation of P during the molecular beam epitaxial growth of Ge and high-concentration active P donors are confined within a few nm of the initial doping position. The current-voltage characteristics of the P δ-doped layers with Si insertion show excellent Ohmic behaviors with low enough resistivity for ultra-shallow Ohmic contacts on n-type Ge. © *2015 AIP Publishing LLC*. [http://dx.doi.org/10.1063/1.4931939]

Metal oxide semiconductor field transistors (MOSFETs) with germanium (Ge) channel have gained much attention as a promising candidate for next generation devices with high mobility. For realization of high-performance n-channel Ge MOSFETs, formation of ultra-shallow Ohmic contacts with low enough resistivity is one of the most important challenges because Schottky barriers are formed irrespective of metal species due to severe Fermi level pinning.[1,2] Insertion of ultra-thin insulators between the metal and Ge reduces the Fermi level pinning;[3–5] however, such insertion of the insulator naturally leads to increase in the contact resistance. Formation of nickel germanide alloys on highly doped Ge also reduces the Fermi level pinning,[6,7] in which high-concentration donor doping is required to obtain low resistivity. To obtain high-concentration doping, ion implantation technique has been conventionally used, which leads to saturation of activated dopants[8,9] and to significant broadening during activation annealing due to concentration dependent diffusivities of n-type dopants in Ge.[10–12] To overcome these difficulties, the δ-doping technique has been investigated because no post growth annealing for activation is needed to achieve high activation of dopants.[13,14] In the δ-doping technique, dopants are deposited with a sub-monolayer thickness during the epitaxial growth of Ge and hence precise control of the dopant depth distribution is possible. However, it has been well known that the donors in Ge tend to segregate towards the growing surface during the growth of further Ge on top of the δ-doped layer.[13,14] Surface segregation in this letter is defined as the segregation of the phosphorous (P) to the surface during the molecular beam epitaxy (MBE) growth of the undoped Ge capping layers. This unintentional segregation not only reduces the peak donor concentration but also broadens the dopant profiles in the depth directions. The suppression of the segregation has been achieved by lowering the growth temperature;[13,15–19] however, the low growth temperatures led to degradation of crystalline quality of the host semiconductor. The segregation of phosphorus during the growth of silicon (Si) is found to be smaller than that of Ge, as will be described below, which leads us to insert Si layers to suppress the P segregation in Ge. In the present study, therefore, insertion of ultra-thin Si layers is utilized to reduce the segregation of P during Ge epitaxial growth. We show that the insertion of Si layers at the P δ-doping region effectively suppresses the P segregation to achieve excellent Ohmic behaviors with low resistivity. In the present study, Ge (111) substrates were used because Ge (111) has higher electron mobility and higher oxide stability than Ge (100),[20] and hence is more useful for realization of high-performance n-channel Ge MOSFETs.

The P δ-doping and Si insertion during the growth of Ge were carried out by solid source MBE on the Ge (111) substrates with the resistivities 30–40 Ω cm. After chemical cleaning by NH_4OH and HF, the substrates were pre-annealed at 700 °C for 10 min in an ultra-high vacuum, and then followed by growth of a 50-nm-thick Ge buffer layer. P was deposited on the buffer layer with the sheet density of 1×10^{14} cm^{-2} (∼0.17 monolayers) at 300 °C using a GaP decomposition Knudsen cell.[21] After the P deposition, an ultra-thin Si insertion layer having thicknesses in the range of 0.2–50 Å was grown at 400 °C with the rate of 0.1 Å/s (0.2–3.3 Å) or 0.5 Å/s (10–50 Å), as shown schematically at the top of Fig. 1. The thickness of Si layer was determined from the growth rate and time. The growth rate was monitored with a crystal quartz sensor calibrated by the thickness of Si/SiGe superlattice structures grown by the MBE, where the thickness is determined by X-ray diffraction measurements. Then, a Ge capping layer with the thickness of 80 nm was grown at temperatures of 300–500 °C with the constant growth rate 0.5 Å/s for all samples. The samples having this structure are labeled A1. In addition, the order of growth for sample A1 was reversed, that is, the Si layer was inserted before the P δ-doping, in order to examine whether the order of layers would change the results. These samples are labeled A2. Samples without Si insertion labeled A3 as control

a)Electronic mail: kitoh@appi.keio.ac.jp

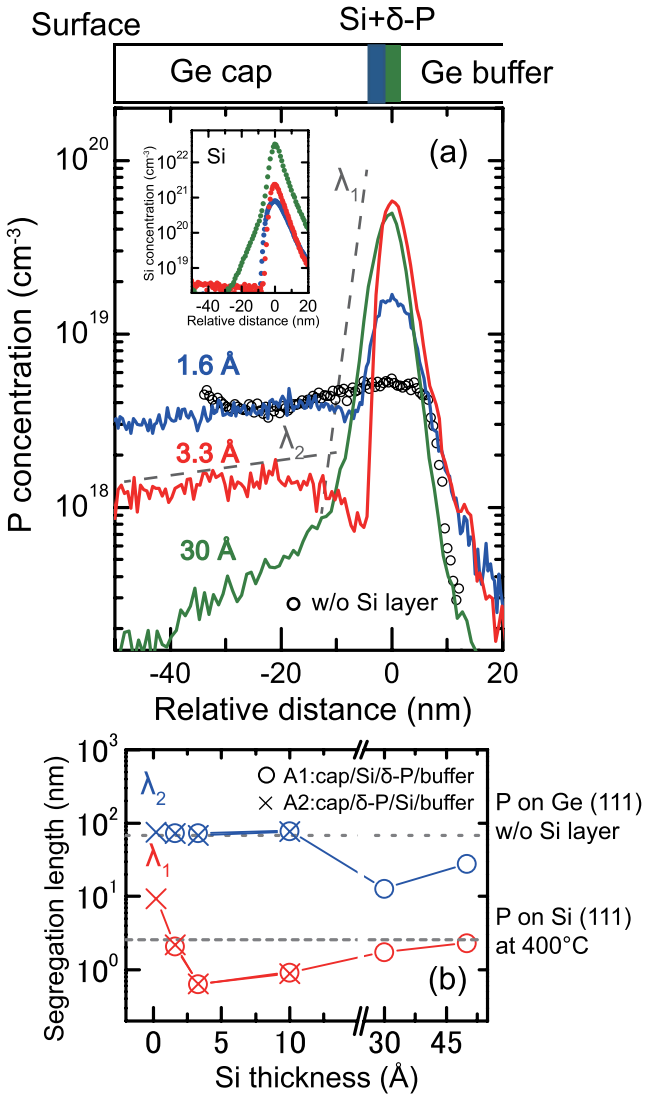

FIG. 1. Results of P δ-doping with $1 \times 10^{14}\,\mathrm{cm}^{-2}$ on Ge (111) at the growth temperature of 400 °C. (a) SIMS depth profiles of P for samples with Si layer insertion after P δ-doping (sample A1). The thicknesses of ultra-thin Si insertion layers are 1.6–30 Å. The inset shows the profiles of Si in the same experiments. The open circles show the P profile when no Si layer was inserted (sample A3). P profiles in sample A2 (not shown in the figure) almost coincide with those in sample A1. Zero in the relative distance is the initial doping position of δ-P. (b) P segregation lengths in the ranges of 0 to −10 nm (λ_1) and −10 to −50 nm (λ_2) as a function of thickness of Si insertion layers (0.2–50 Å). Open circles show the lengths in samples with Si layer insertion after P δ-doping (sample A1) and crosses present those before the doping (sample A2). The broken lines show the P segregation lengths during homoepitaxial growth on δ-doped Ge (111) [sample A3: the upper line] and on Si (111) [the lower line] at 400 °C. The lines are guide to the eyes and are offset for clarity in the horizontal axis.

samples are also prepared. For the measurements of current-voltage (I-V) characteristics, samples A2 and A3 were used, in which a 15 nm-thick-capping layer was grown at 300 °C and the buffer layer was uniformly and lightly ($\sim 10^{17}\,\mathrm{cm}^{-3}$) P-doped so that the layer is n-type. The depth profiles of P and Si were investigated by secondary ion mass spectrometry (SIMS) using Cs^+ primary ions with an acceleration energy of 1 keV. The crystalline quality of the Si layer and the Ge capping layer was observed by cross-sectional transmission microscopy (XTEM). The I-V characteristics were investigated by depositing Au/Ti to form Schottky diodes. Au/Ti pads of the diameter 100 μm were formed by vacuum deposition after removing the native oxide at the top. Backside Ohmic contacts were prepared by depositing AuSb alloys.

Fig. 1(a) shows the SIMS depth profiles of P for samples with Si layer insertion after P δ-doping and the inset represents the profiles of Si (sample A1). The P profile of the control sample, that is, without Si insertion (sample A3) is also shown in the figure. The capping layer was grown at 400 °C for all samples. The horizontal axis represents the relative distance from the P δ-doping position. In the control sample A3 (without Si insertion), P atoms strongly segregate towards the surface during the growth, and no sharp P profiles are observed at the initial doping position. Note that the P profiles are not significantly broadened toward the substrate, which indicates that the broadening toward the surface is mainly caused by the surface segregation and that the influence of P diffusion during the growth at 400 °C is minor. On the other hand, for sample A1 (with Si insertion), the segregation of P is significantly suppressed and the P atoms are confined within a few nm at the initial doping position. Especially with increasing the Si layer thickness from 1.6 to 3.3 Å, the suppression becomes more significant and the P peak concentration remarkably increases. Note that the actual P profiles are more abrupt than those in Fig. 1(a) and the smearing of the P profiles is due to the SIMS artifact (knock-on mixing, etc.).[22] In Fig. 1(a), two different slopes of the P concentration are observed in the ranges of 0 to −10 nm and −10 to −50 nm in sample A1. In the range of 0 to −10 nm, the Si concentration (see the inset) is much higher than $10^{20}\,\mathrm{cm}^{-3}$ and the P segregation is suppressed. In contrast, in the range of −10 to −50 nm, where the Si concentration is below $10^{20}\,\mathrm{cm}^{-3}$, the suppression of P segregation by Si is much weakened and the slope of the P concentration becomes small. Note that the P profile in this range is similar to that in sample A3 [without Si insertion; open circles in Fig. 1(a)]. These results imply that most of the Si atoms remain at the growing surface and the content of Si greatly reduces the P segregation to efficiently incorporate P atoms. The same tendency was observed for sample A2, in which the Si layer was inserted before the P δ-doping, reversing the order of growth for sample A1. In order to quantify the degree of segregation, we estimate the segregation length, which is defined as the length from the peak to the concentration 1/e. The segregation length, in general, is uniquely given for a given material at given growth temperature, growth rate, and substrate orientation, and hence, the length is uniquely determined in the same condition. The P segregation lengths in the ranges of 0 to −10 nm (λ_1) and −10 to −50 nm (λ_2) in sample A1 are obtained from the two different slopes, as schematically shown in Fig. 1(a). The λ_1 and λ_2 correspond to the segregation lengths in the regions with high and low Si concentration, respectively. The P segregation lengths λ_1 and λ_2 in sample A1 are plotted as a function of Si layer thickness in Fig. 1(b), where those in sample A2 are also plotted. The λ_1 decreases drastically with the increase of Si layer thickness up to ~3.3 Å. Here the P segregation length λ_1 with the Si thickness of 3.3 Å is estimated to be 0.6 nm, which is smaller than 4.0 nm of antimony (Sb) in Ge without Si insertion.[13] When the Si layer is thicker than ~10 Å, the λ_1 then gradually increases to reach the P

segregation length during Si growth on Si (111) at 400 °C. This P segregation length during Si homoepitaxial growth was obtained in this study under the same growth conditions as for sample A1 and is presented by the lower broken line in Fig. 1(b). For the λ_2, it is almost constant up to ~10 Å and is very close to the P segregation length without Si insertion obtained from sample A3, which is presented by the upper broken line. When the Si insertion layer is thinner than ~10 Å, the Si concentration is below $10^{19}\,cm^{-3}$ in the range of −10 to −50 nm [the inset of Fig. 1(a)], and hence, the suppression of P segregation by Si is much weakened. In contrast, when the Si insertion layer is thicker than ~30 Å, the Si concentration of higher than $10^{19}\,cm^{-3}$ exists in the range of −10 to −50 nm [the inset of Fig. 1(a)], where the P segregation is suppressed by Si, and therefore, the λ_2 decreases with the increase of Si layer thickness from 10 to 30 Å. Samples A1 and A2 show almost the same segregation lengths, and in addition, the P profiles in sample A2 (not shown in the figure) almost coincide with those in sample A1, which are shown in Fig. 1(a). This suggests that there may be a rapid mixing of P and Si at the growing surface when the Si layer is thinner than at least 10 Å.

Figure 2 shows the images of XTEM of sample A1 with the Si layer thicknesses of 3.3−50 Å. For the 3.3 Å sample, no dislocations were observed; however, with increasing the thickness, more misfit dislocations are generated in the Si layer and the Ge capping layer. The results indicate that the Si insertion of ~2 monolayers (3.3 Å) is optimum for both the suppression of segregation and high crystalline quality. Figure 3 shows the P segregation lengths λ_1 and λ_2 in sample A1 as a function of growth temperature when the Si layer thickness is 3.3 Å. The P segregation lengths without insertion (sample A3) are also represented. The values of λ_1 with Si insertion are significantly smaller than the segregation length without Si insertion. In contrast, the values of λ_2 with

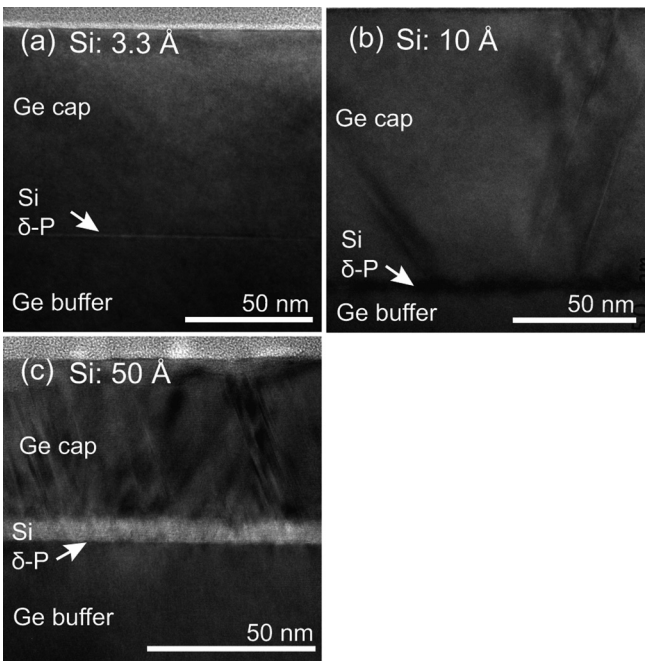

FIG. 2. XTEM images of sample A1 with the Si layer thicknesses of (a) 3.3, (b) 10, and (c) 50 Å.

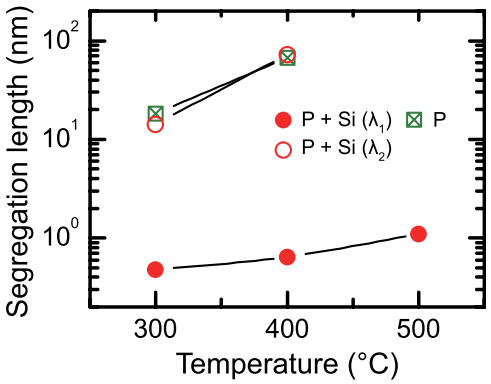

FIG. 3. Circles show P segregation lengths of sample A1 in the ranges of 0 to −10 nm (λ_1) and −10 to −50 nm (λ_2) [see Fig. 1(a)] as a function of growth temperature when the Si layer thickness is 3.3 Å. Squares represent P segregation lengths without insertion (sample A3). The lines are guide to the eyes.

Si insertion are almost the same as the segregation length without Si insertion. This is attributed to small Si segregation toward the surface and hence the Si concentration in the range of 0 to −10 nm is high enough to suppress the P segregation. In the range of −10 to −50 nm, the Si concentration is so small that the P segregation length becomes close to that without Si insertion. This indicates that the Si content plays an important role for reducing the P segregation. Note that the value of λ_1 with Si insertion is as small as 1 nm even at the growth temperature of 500 °C. In contrast, in sample A3 (without Si insertion grown at 500 °C), a weak signature of diffusion of P atoms towards the substrate by the heating during the growth was seen (not shown in the figure). This indicates that the abrupt P profiles around Si layers are thermally stable and the Si layer acts as a P diffusion barrier, as has been shown in the previous report.[23]

The λ_1 decreases drastically with the increase of Si layer thickness up to ~3.3 Å, as shown in Fig. 1(b). This abrupt decrease is partly attributed to the Si content in the P δ−doping layer because the segregation of P in Si is smaller than that in Ge [see Fig. 1(b)]. However, this cannot explain the gradual increase of λ_1 with the Si layer thicker than ~10 Å. As described above, with the insertion of thick Si layers, misfit dislocations are generated, which may relax the strain induced by the lattice mismatch between Ge and Si.[24] The strain due to lattice mismatch affects the dopant segregation during growth and Portavoce *et al.*[25] showed that compressive strain in SiGe enhances the segregation of Sb. This result allows us to assume that tensile strain may retard P segregation. In our experiments, the inserted thin Si layers are tensely strained on Ge. Therefore, the suppression of P segregation by the Si insertion can be explained not only due to Si content but also due to tensile strain. As the strain of Si layers is relaxed by the generation of misfit dislocations (see Fig. 2), the strain effect is weakened and the segregation length λ_1 becomes close to that during the Si growth on Si (111), as seen in Fig. 1(b). Misfit dislocations may act as a sink for P in a similar manner that Al segregates around dislocations during the growth of AlGaN.[26] Then the P segregation would be suppressed with thicker Si layers having more dislocations; however, the P segregation increases with the Si layer thicker than ~10 Å in our experiment. These results

imply that the influence of dislocations acting as a sink for P is minor compared with that of strain on the P segregation. For other substrate orientations, the surfaces have different structures and hence different behaviors of segregation may be observed;[13,16,19] however, the strain due to lattice mismatch has been observed in SiGe layers grown on (100), (110), and (111) Si substrates.[27] This implies that the strain which suppresses P segregation by Si insertion exists regardless of Ge substrate orientations. It can therefore be presumed that the Si insertion effect observed in our study is also observed for other substrate orientations such as Ge (100).

Figure 4(a) shows the I-V characteristics of Au/Ti/n-Ge Schottky diodes that are un-doped and P δ-doped with Si insertion of 3.3 Å thicknesses (sample A2) and without insertion (A3). We used the samples with the thickness of 3.3 Å because they have the smallest segregation length and high crystalline quality, as shown in Figs. 1 and 2. The thickness of capping layers was reduced to 15 nm so that the position of δ-doping is closer to that of Schottky junction. For the sample with Si insertion, Ohmic behaviors with low resistivity are obtained. This is attributed to small Si segregation during the growth, as described above, and therefore, the concentration of Si around the P δ-doping layer is high enough to effectively suppress P segregation. In addition, no misfit dislocations were observed by TEM in this 3.3-Å-thick sample, as shown in Fig. 2(a). For the sample without insertion of Si (A3), the linear I-V plot in the inset shows incomplete Ohmic conductance, that is, straight lines with different slopes in the forward and reverse bias regions. For the undoped sample, rectifying behavior is observed due to the Schottky barrier. To investigate the tunneling phenomena in the transport, the temperature dependence of the I-V characteristics is investigated. Figure 4(b) shows the current density at a reverse bias of −0.1 V as a function of measurement temperature from 175 to 300 K for the samples with Si insertion of 3.3 Å thicknesses (A2). No significant reduction of the current with the decrease in temperature is observed, which obviously demonstrates that the conduction via tunneling is dominant in the reverse bias region owing to the high-concentration doping of activated P donors.

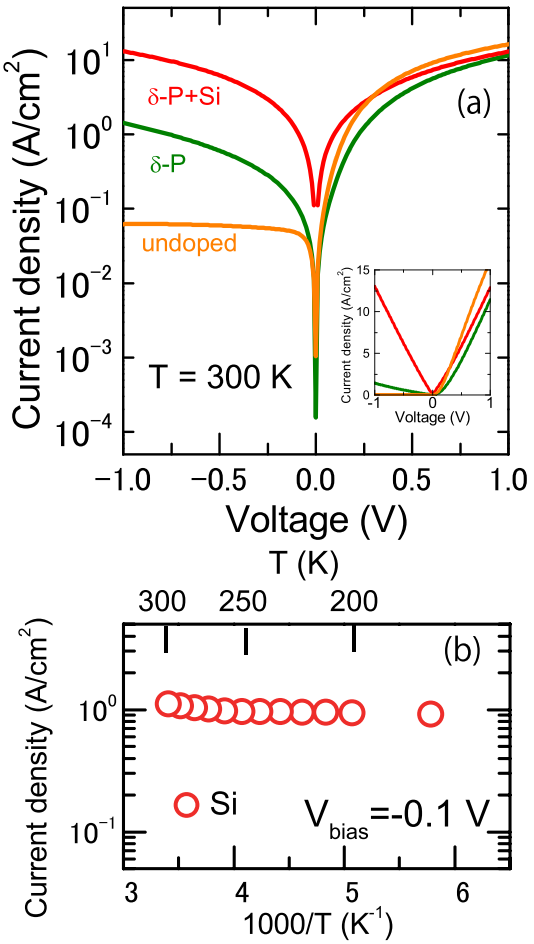

FIG. 4. (a) Room temperature I-V characteristics for Au/Ti/n-Ge Schottky diodes that are un-doped and P δ-doped with 3.3-Å-thick Si insertion (sample A2) and without insertion (sample A3). The thickness of capping layers is 15 nm and the growth temperature is 300 °C. The inset shows the linear plot of I-V characteristics. (b) Current density at a reverse bias of −0.1 V as a function of measurement temperature from 175 to 300 K for the Schottky diode that is P δ-doped with Si insertion.

In summary, we have shown that the insertion of ultra-thin Si layers effectively suppresses the P segregation during Ge growth. Abrupt profiles of high-concentration δ-doping of active P donors were formed at the initial doping position. When the Si layer thickness is ∼2 monolayers (3.3 Å), the segregation length as small as 0.6 nm was obtained, where no misfit dislocations were observed by TEM. The I-V measurements of Au/Ti/n-Ge Schottky diodes with the P δ-doped layers showed excellent Ohmic behaviors, in which tunneling conduction through Schottky barriers is dominant. The present results show that P δ-doping with the insertion of ultra-thin Si layers is a useful technique to obtain ultra-shallow Ohmic contacts on n-type Ge.

This work was supported in parts by the Grant-in-Aid for Scientific Research by MEXT, NanoQuine, JSPS Core-to-Core Program, and Cooperative Research Project Program of the RIEC, Tohoku University.

[1]T. Nishimura, K. Kita, and A. Toriumi, Appl. Phys. Lett. **91**, 123123 (2007).
[2]A. Dimoulas, P. Tsipas, A. Sotiropoulos, and E. K. Evangelou, Appl. Phys. Lett. **89**, 252110 (2006).
[3]Y. Zhou, M. Ogawa, X. Han, and K. L. Wang, Appl. Phys. Lett. **93**, 202105 (2008).
[4]R. R. Lieten, S. Degroote, M. Kuijk, and G. Borghs, Appl. Phys. Lett. **92**, 022106 (2008).
[5]T. Nishimura, K. Kita, and A. Toriumi, Appl. Phys. Express **1**, 051406 (2008).
[6]K. Ikeda, Y. Yamashita, N. Sugiyama, N. Taoka, and S. Takagi, Appl. Phys. Lett. **88**, 152115 (2006).
[7]T. Nishimura, S. Sakata, K. Nagashio, K. Kita, and A. Toriumi, Appl. Phys. Express **2**, 021202 (2009).
[8]C. O. Chui, L. Kulig, J. Moran, W. Tsai, and K. C. Saraswat, Appl. Phys. Lett. **87**, 091909 (2005).
[9]A. Satta, E. Simoen, R. Duffy, T. Janssens, T. Clarysse, A. Benedetti, M. Meuris, and W. Vandervorst, Appl. Phys. Lett. **88**, 162118 (2006).
[10]S. Matsumoto and T. Niimi, J. Electrochem. Soc. **125**, 1307 (1978).
[11]M. Naganawa, Y. Shimizu, M. Uematsu, K. M. Itoh, K. Sawano, Y. Shiraki, and E. E. Haller, Appl. Phys. Lett. **93**, 191905 (2008).
[12]S. Brotzmann and H. Bracht, J. Appl. Phys. **103**, 033508 (2008).
[13]K. Sawano, Y. Hoshi, K. Kasahara, K. Yamane, K. Hamaya, M. Miyao, and Y. Shiraki, Appl. Phys. Lett. **97**, 162108 (2010).
[14]G. Scappucci, G. Capellini, W. C. T. Lee, and M. Y. Simmons, Appl. Phys. Lett. **94**, 162106 (2009).
[15]G. Scappucci, G. Capellini, and M. Y. Simmons, Phys. Rev. B **80**, 233202 (2009).
[16]J. F. Nutzel and G. Abstreiter, Phys. Rev. B **53**, 13551 (1996).

[17]P. E. Thompson and G. G. Jernigan, Semicond. Sci. Technol. **22**, S80 (2007).
[18]E. Friess, J. Nuützel, and G. Abstreiter, Appl. Phys. Lett. **60**, 2237 (1992).
[19]K. Nakagawa and M. Miyao, Thin Solid Films **183**, 315 (1989).
[20]C. H. Lee, T. Nishimura, N. Saido, K. Nagashio, K. Kita, and A. Toriumi, Tech. Dig.–Int. Electron Devices Meet. **2009**, 457.
[21]G. Lippert, H. J. Osten, D. Kruüger, P. Gaworzewski, and K. Eberl, Appl. Phys. Lett. **66**, 3197 (1995).
[22]Y. Shimizu, M. Uematsu, K. M. Itoh, A. Takano, K. Sawano, and Y. Shiraki, Appl. Phys. Express **1**, 021401 (2008).
[23]Y. Yamamoto, P. Zaumseil, J. Murota, and B. Tillack, ECS J. Solid State Sci. Technol. **3**, P1 (2014).
[24]W. Wegscheide, K. Eberl, G. Abstreiter, H. Cerva, and H. Oppolzer, Appl. Phys. Lett. **57**, 1496 (1990).
[25]A. Portavoce, I. Berbezier, P. Gas, and A. Ronda, Phys. Rev. B **69**, 155414 (2004).
[26]L. Chang, S. K. Lai, F. R. Chen, and J. J. Kai, Appl. Phys. Lett. **79**, 928 (2001).
[27]A. Zhylik, A. Benediktovich, A. Ulyanenkov, H. Guerault, M. Myronov, A. Dobbie, D. R. Leadley, and T. Ulyanenkova, J. Appl. Phys. **109**, 123714 (2011).